Politecnico di Bari

Repository Istituzionale dei Prodotti della Ricerca del Politecnico di Bari

Observation of an excess in the search for the Standard Model Higgs boson at ALEPH

This is a post print of the following article

Original Citation:
Observation of an excess in the search for the Standard Model Higgs boson at ALEPH / Barate, R., De Bonis, I., Decamp, D., Ghez, P., Goy, C., Jezequel, S., Lees, J.p., Martin, F., Merle, E., Minard, M.n., Pietrzyk, B., Bravo, S., Casado, M.p., Chmeissani, M., Crespo, J.m., Fernandez, E., Fernandez Bosman, M., Garrido, L., Grauges, E., Lopez, J., et al.. - In: PHYSICS LETTERS. SECTION B. - ISSN 0370-2693. - STAMPA. - 495:1-2(2000), pp. 1-17. [10.1016/S0370-2693(00)01269-7]

Availability:
This version is available at http://hdl.handle.net/11589/3605 since:

Published version
DOI:10.1016/S0370-2693(00)01269-7

Publisher:

Terms of use:

(Article begins on next page)

09 October 2026

ELSEVIER

7 December 2000

PHYSICS LETTERS B

Physics Letters B 495 (2000) 1–17

www.elsevier.nl/locate/npe

Observation of an excess in the search for the Standard Model Higgs boson at ALEPH

ALEPH Collaboration

R. Barate, I. De Bonis, D. Decamp, P. Ghez, C. Goy, S. Jezequel, J.-P. Lees, F. Martin, E. Merle, M.-N. Minard, B. Pietrzyk

Laboratoire de Physique des Particules (LAPP), IN^{2}P^3-CNRS, F-74019 Annecy-le-Vieux Cedex, France

S. Bravo, M.P. Casado, M. Chmeissani, J.M. Crespo, E. Fernandez, M. Fernandez-Bosman, Ll. Garrido [1], E. Graugés, J. Lopez, M. Martinez, G. Merino, R. Miquel, Ll.M. Mir, A. Pacheco, D. Paneque, H. Ruiz

Institut de Física d'Altes Energies, Universitat Autònoma de Barcelona, E-08193 Bellaterra (Barcelona), Spain [2]

A. Colaleo, D. Creanza, N. De Filippis, M. de Palma, G. Iaselli, G. Maggi, M. Maggi [3], S. Nuzzo, A. Ranieri, G. Raso [4], F. Ruggieri, G. Selvaggi, L. Silvestris, P. Tempesta, A. Tricomi [5], G. Zito

Dipartimento di Fisica, INFN Sezione di Bari, I-70126 Bari, Italy

X. Huang, J. Lin, Q. Ouyang, T. Wang, Y. Xie, R. Xu, S. Xue, J. Zhang, L. Zhang, W. Zhao

Institute of High Energy Physics, Academia Sinica, Beijing, People's Republic of China [6]

D. Abbaneo, P. Azzurri, T. Barklow [7], G. Boix [8], O. Buchmüller, M. Cattaneo, F. Cerutti, B. Clerbaux, G. Dissertori, H. Drevermann, R.W. Forty, M. Frank, F. Gianotti, T.C. Greening, J.B. Hansen, J. Harvey, D.E. Hutchcroft, P. Janot, B. Jost, M. Kado, V. Lemaitre, P. Maley, P. Mato, A. Minten, A. Moutoussi, F. Ranjard, L. Rolandi, D. Schlatter M. Schmitt [9], O. Schneider [10], P. Spagnolo, W. Tejessy, F. Teubert, E. Tournefier [11], A. Valassi, J.J. Ward, A.E. Wright

European Laboratory for Particle Physics (CERN), CH-1211 Geneva 23, Switzerland

Z. Ajaltouni, F. Badaud, S. Dessagne, A. Falvard, D. Fayolle, P. Gay, P. Henrard, J. Jousset, B. Michel, S. Monteil, J.-C. Montret, D. Pallin, J.M. Pascolo, P. Perret, F. Podlyski

Laboratoire de Physique Corpusculaire, Université Blaise Pascal, IN^{2}P^3-CNRS, Clermont-Ferrand, F-63177 Aubière, France

0370-2693/00/$ – see front matter © 2000 Elsevier Science B.V. All rights reserved.
PII: S0370-2693(00)01269-7

J.D. Hansen, J.R. Hansen, P.H. Hansen, B.S. Nilsson, A. Wäänänen

Niels Bohr Institute, 2100 Copenhagen, Denmark [12]

G. Daskalakis, A. Kyriakis, C. Markou, E. Simopoulou, A. Vayaki

Nuclear Research Center Demokritos (NRCD), GR-15310 Attiki, Greece

A. Blondel [13], J.-C. Brient, F. Machefert, A. Rougé, M. Swynghedauw, R. Tanaka, H. Videau

Laboratoire de Physique Nucléaire et des Hautes Energies, Ecole Polytechnique, IN^{2}P^3-CNRS, F-91128 Palaiseau Cedex, France

E. Focardi, G. Parrini, K. Zachariadou

Dipartimento di Fisica, Università di Firenze, INFN Sezione di Firenze, I-50125 Firenze, Italy

A. Antonelli, M. Antonelli, G. Bencivenni, G. Bologna [14], F. Bossi, P. Campana, G. Capon, V. Chiarella, P. Laurelli, G. Mannocchi [15], F. Murtas, G.P. Murtas, L. Passalacqua, M. Pepe-Altarelli [16]

Laboratori Nazionali dell'INFN (LNF-INFN), I-00044 Frascati, Italy

M. Chalmers, A.W. Halley, J. Kennedy, J.G. Lynch, P. Negus, V. O'Shea, B. Raeven, D. Smith, P. Teixeira-Dias, A.S. Thompson

Department of Physics and Astronomy, University of Glasgow, Glasgow G12 8QQ, UK [17]

R. Cavanaugh, S. Dhamotharan, C. Geweniger, P. Hanke, V. Hepp, E.E. Kluge, G. Leibenguth, A. Putzer, K. Tittel, S. Werner [18], M. Wunsch [18]

Kirchhoff-Institut für Physik, Universität Heidelberg, D-69120 Heidelberg, Germany [19]

R. Beuselinck, D.M. Binnie, W. Cameron, G. Davies, P.J. Dornan, M. Girone [3], N. Marinelli, J. Nowell, H. Przysiezniak, J.K. Sedgbeer, J.C. Thompson [20], E. Thomson [21], R. White

Department of Physics, Imperial College, London SW7 2BZ, UK [17]

V.M. Ghete, P. Girtler, E. Kneringer, D. Kuhn, G. Rudolph

Institut für Experimentalphysik, Universität Innsbruck, A-6020 Innsbruck, Austria [22]

E. Bouhova-Thacker, C.K. Bowdery, D.P. Clarke, G. Ellis, A.J. Finch, F. Foster, G. Hughes, R.W.L. Jones [3], M.R. Pearson, N.A. Robertson, M. Smizanska

Department of Physics, University of Lancaster, Lancaster LA1 4YB, UK [17]

I. Giehl, F. Hölldorfer, K. Jakobs, K. Kleinknecht, M. Kröcker, A.-S. Müller, H.-A. Nürnberger, G. Quast [3], B. Renk, E. Rohne, H.-G. Sander, S. Schmeling, H. Wachsmuth, C. Zeitnitz, T. Ziegler

Institut für Physik, Universität Mainz, D-55099 Mainz, Germany [19]

A. Bonissent, J. Carr, P. Coyle, C. Curtil, A. Ealet, D. Fouchez, O. Leroy, T. Kachelhoffer, P. Payre, D. Rousseau, A. Tilquin

Centre de Physique des Particules de Marseille, Univ Méditerranée, IN^{2}P^3-CNRS, F-13288 Marseille, France

M. Aleppo, S. Gilardoni, F. Ragusa

Dipartimento di Fisica, Università di Milano e INFN Sezione di Milano, I-20133 Milano, Italy

A. David, H. Dietl, G. Ganis [23], A. Heister, K. Hüttmann, G. Lütjens, C. Mannert, W. Männer, H.-G. Moser, S. Schael, R. Settles [3], H. Stenzel, G. Wolf

Max-Planck-Institut für Physik, Werner-Heisenberg-Institut, D-80805 München, Germany [19]

J. Boucrot [3], O. Callot, M. Davier, L. Duflot, J.-F. Grivaz, Ph. Heusse, A. Jacholkowska [3], L. Serin, J.-J. Veillet, I. Videau, J.-B. de Vivie de Régie [24], C. Yuan, D. Zerwas

Laboratoire de l'Accélérateur Linéaire, Université de Paris-Sud, IN^{2}P^3-CNRS, F-91898 Orsay Cedex, France

G. Bagliesi, T. Boccali, G. Calderini, V. Ciulli, L. Foà, A. Giammanco, A. Giassi, F. Ligabue, A. Messineo, F. Palla [3], G. Rizzo, G. Sanguinetti, A. Sciabà, G. Sguazzoni, J. Steinberger, R. Tenchini [3], A. Venturi, P.G. Verdini

Dipartimento di Fisica dell'Università, INFN Sezione di Pisa, e Scuola Normale Superiore, I-56010 Pisa, Italy

G.A. Blair, J. Coles, G. Cowan, M.G. Green, L.T. Jones, T. Medcalf, J.A. Strong

Department of Physics, Royal Holloway & Bedford New College, University of London, Surrey TW20 OEX, UK [17]

R.W. Clifft, T.R. Edgecock, P.R. Norton, I.R. Tomalin

Particle Physics Department, Rutherford Appleton Laboratory, Chilton, Didcot, Oxon OX11 OQX, UK [17]

B. Bloch-Devaux [3], D. Boumediene, P. Colas, B. Fabbro, E. Lançon, M.-C. Lemaire, E. Locci, P. Perez, J. Rander, J.-F. Renardy, A. Rosowsky, P. Seager [25], A. Trabelsi [26], B. Tuchming, B. Vallage

CEA, DAPNIA/Service de Physique des Particules, CE-Saclay, F-91191 Gif-sur-Yvette Cedex, France [27]

N. Konstantinidis, C. Loomis, A.M. Litke, G. Taylor

Institute for Particle Physics, University of California at Santa Cruz, Santa Cruz, CA 95064, USA [28]

C.N. Booth, S. Cartwright, F. Combley, P.N. Hodgson, M. Lehto, L.F. Thompson

Department of Physics, University of Sheffield, Sheffield S3 7RH, UK [17]

K. Affholderbach, A. Böhrer, S. Brandt, C. Grupen, J. Hess, A. Misiejuk, G. Prange, U. Sieler

Fachbereich Physik, Universität Siegen, D-57068 Siegen, Germany [19]

C. Borean, G. Giannini, B. Gobbo

Dipartimento di Fisica, Università di Trieste e INFN Sezione di Trieste, I-34127 Trieste, Italy

H. He, J. Putz, J. Rothberg, S. Wasserbaech

Experimental Elementary Particle Physics, University of Washington, Seattle, WA 98195, USA

S.R. Armstrong, K. Cranmer, P. Elmer, D.P.S. Ferguson, Y. Gao [29], S. González, O.J. Hayes, H. Hu, S. Jin, J. Kile, P.A. McNamara III, J. Nielsen, W. Orejudos, Y.B. Pan, Y. Saadi, I.J. Scott, N. Shao, J.H. von Wimmersperg-Toeller, J. Walsh, W. Wiedenmann, J. Wu, S.L. Wu, X. Wu, G. Zobernig

Department of Physics, University of Wisconsin, Madison, WI 53706, USA [30]

Received 10 November 2000; accepted 13 November 2000
Editor: L. Montanet

Abstract

A search has been performed for the Standard Model Higgs boson in the data sample collected with the ALEPH detector at LEP, at centre-of-mass energies up to 209 GeV. An excess of 3σ beyond the background expectation is found, consistent with

[1] Permanent address: Universitat de Barcelona, 08208 Barcelona, Spain.
[2] Supported by CICYT, Spain.
[3] Also at CERN, 1211 Geneva 23, Switzerland.
[4] Also at Dipartimento di Fisica e Tecnologie Relative, Università di Palermo, Palermo, Italy.
[5] Also at Dipartimento di Fisica di Catania and INFN Sezione di Catania, 95129 Catania, Italy.
[6] Supported by the National Science Foundation of China.
[7] Also at SLAC, Stanford, CA 94309, USA.
[8] Supported by the Commission of the European Communities, contract ERBFMBICT982894.
[9] Now at Harvard University, Cambridge, MA 02138, USA.
[10] Now at Université de Lausanne, 1015 Lausanne, Switzerland.
[11] Now at ISN, Institut des Sciences Nucléaires, 53 Av. des Martyrs, 38026 Grenoble, France.
[12] Supported by the Danish Natural Science Research Council.
[13] Now at Departement de Physique Corpusculaire, Université de Genève, 1211 Genève 4, Switzerland.
[14] Deceased.
[15] Also Istituto di Cosmo-Geofisica del C.N.R., Torino, Italy.
[16] Now at CERN, 1211 Geneva 23, Switzerland.
[17] Supported by the UK Particle Physics and Astronomy Research Council.
[18] Now at SAP AG, 69185 Walldorf, Germany.
[19] Supported by the Bundesministerium für Bildung, Wissenschaft, Forschung und Technologie, Germany.
[20] Also at Rutherford Appleton Laboratory, Chilton, Didcot, UK.
[21] Now at Department of Physics, Ohio State University, Columbus, OH 43210-1106, USA.
[22] Supported by the Austrian Ministry for Science and Transport.
[23] Now at Università degli Studi di Roma Tor Vergata, Dipartimento di Fisica, 00133 Roma, Italy.
[24] Now at Centre de Physique des Particules de Marseille, Univ. Méditerranée, F-13288 Marseille, France.
[25] Supported by the Commission of the European Communities, contract ERBFMBICT982874.
[26] Now at Département de Physique, Faculté des Sciences de Tunis, 1060 Le Belvédère, Tunisia.
[27] Supported by the Direction des Sciences de la Matière, C.E.A.
[28] Supported by the US Department of Energy, grant DE-FG03-92ER40689.
[29] Also at Department of Physics, Tsinghua University, Beijing, The People's Republic of China.
[30] Supported by the US Department of Energy, grant DE-FG0295-ER40896.

the production of the Higgs boson with a mass near 114 GeV/c^2. Much of this excess is seen in the four-jet analyses, where three high purity events are selected. © 2000 Elsevier Science B.V. All rights reserved.

1. Introduction

This Letter presents results on the search for the Standard Model Higgs boson [1] using the data collected by ALEPH at LEP in the year 2000. Similar analyses on previous years' data, with centre-of-mass energies up to 202 GeV, have shown no evidence for a signal [2]. A lower mass limit of 107.7 GeV/c^2 was set at the 95% confidence level.

The ALEPH detector, described fully in Ref. [3], is a general purpose detector composed of tracking, vertexing, and calorimetry subdetectors. This search looks for a Higgs boson produced in association with a Z boson through the Higgsstrahlung process, $e^+e^- \to HZ$ [4]. This process is supplemented by a small contribution from the W and Z vector boson fusion processes, which produce a Higgs boson and either a pair of neutrinos or electrons in the final state [5]. The Feynman diagrams for these processes are shown in Fig. 1.

The centre-of-mass energies for the 216.1 pb^{-1} of data collected in the year 2000 range from 200 GeV to 209 GeV, with the majority of the data collected around 205.1 GeV (72 pb^{-1}) and 206.7 GeV (107 pb^{-1}). Fig. 2 shows the number of Higgs boson events expected to be produced in this sample as a function of the Higgs boson mass. For a mass of 114 GeV/c^2, 14.4 signal events are expected to be produced. The Higgs boson at this mass predominantly decays into $b\bar{b}$ quark pairs (74%) and tau lepton pairs (7%). The overall selection efficiency is typically 50%.

The purpose of this Letter is to report the observation of an excess which is consistent with the production of the Standard Model Higgs boson with a mass near 114 GeV/c^2. These results are based upon events reconstructed using preliminary detector calibrations. The results obtained after the final event processing, a possible reoptimization of some analyses, and a more detailed investigation of systematic effects, will be reported in a forthcoming publication. It has been verified that the significance of the most signal-like events is not affected by the final processing.

2. Event selection

The analyses designed to search for the Standard Model Higgs boson address most of the final states arising from the reaction $e^+e^- \to HZ$: the four-jet final state ($Hq\bar{q}$), the missing energy final state ($H\nu\bar{\nu}$), the lepton pair final state ($H\ell^+\ell^-$ where ℓ denotes an electron or muon), and the tau lepton final state ($H\tau^+\tau^-$ and $H \to \tau^+\tau^-$, $Z \to q\bar{q}$). As in Ref. [2], the Higgs boson search was conducted using both a neural-network-based stream (denoted "NN") and a cut-based stream ("cut"). Alternative analyses are used in the searches for four-jet and for missing energy final states, while the searches are identical in both streams for the lepton pair and tau lepton final states. All of the analysis selection criteria for the results presented here were fixed before the data taking period began.

These analyses follow closely those designed for the data collected in 1999 [2]. In particular, the b tagging neural network described in Ref. [6] is used, based upon the b-hadron lifetime, mass and semi-leptonic decays. Its output ranges from 0 to 1, where a value of 1 indicates a well b tagged jet. The four-jet and tau lepton final state analyses are identical to those of 1999, while the missing energy and lepton pair final state analyses have had the following improvements:

- The two neural network analyses used in the search for the missing energy final state in the NN stream have been replaced by a single neural network with three output classes. This neural network is trained to identify three types of events: the signal, the $q\bar{q}$ background, and the W^+W^- background. With this technique the benefits of the two previous approaches are merged without any loss in performance.
- The missing energy analysis for the cut stream has an improved rejection of three-jet events from the $q\bar{q}g(\gamma)$ and $q\bar{q}\gamma(\gamma)$ processes. A jet algorithm [7] is applied to form three jets. Events from $q\bar{q}g(\gamma)$ are removed by cuts on the minimum angle and on the minimum distance [7] between any two jets. Three-jet events originating from the $q\bar{q}\gamma(\gamma)$ process with

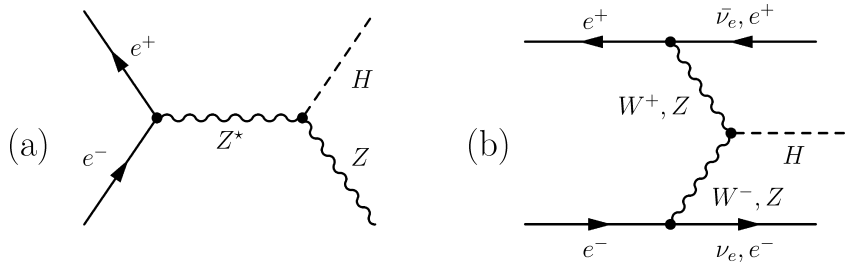

Fig. 1. Feynman diagrams of Higgs boson production at LEP through the (a) Higgsstrahlung and (b) gauge boson fusion processes.

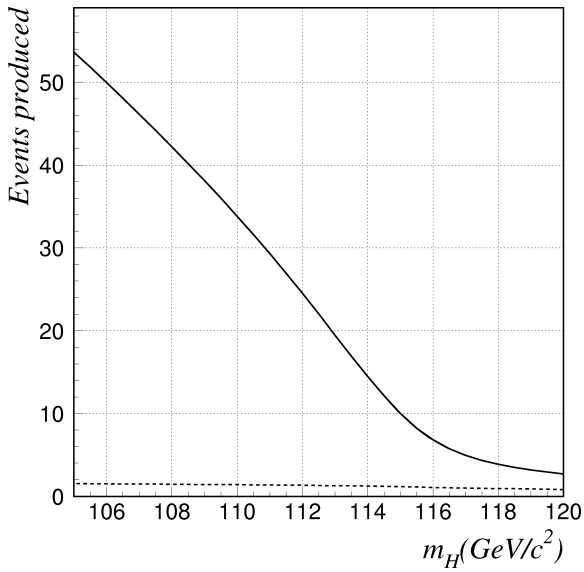

Fig. 2. The expected number of Standard Model Higgs boson events produced in the year 2000 data as a function of the Higgs boson mass (solid curve). The dashed curve shows the contribution of the boson fusion processes, including their interference with the Higgsstrahlung process.

a photon in the detector are removed if any of the three jets is predominantly electromagnetic in origin.

- The analysis for the lepton pair final state has three improvements: (1) an increased efficiency in the identification of events in which the Higgs boson decays to τ leptons, (2) reduced expected background for events with isolated photons, and (3) an increased sensitivity above the nominal kinematic limit, achieved by relaxing requirements on the measured Z boson mass.

The four-jet NN and cut analyses differ in their method to choose the best jet pairing. The four-jet cut analysis chooses the pairing, as described in Ref. [8], based upon the decay angles of the Z and Higgs bosons. The NN analysis includes these two variables in the neural network and selects the jet pairing with the largest neural network output value, thereby effectively also using the b tagging and Z boson mass information.

In the four-jet analysis, a 4C-kinematic fit is performed, in which energy and momentum conservation are imposed. The reconstructed Higgs boson mass m_{REC} is calculated as $m_{12} + m_{34} - m_{\mathrm{Z}}$, where m_{12} and m_{34} are the fitted Z and Higgs boson masses. In the missing energy final state, the Higgs boson mass is reconstructed by a rescaling of the hadronic jets such that the missing mass is the Z boson mass. In the lepton pair final state, it is calculated as the mass recoiling against the pair of leptons. In the tau lepton final state, it results from a kinematic fit, with the Z mass constraint imposed either on the tau pair or on the hadronic system.

Fully simulated samples of signal and background processes were produced with the same generators used in Ref. [2]. The sizes of the simulated samples correspond to at least 50 times the collected luminosity. For each analysis, the expected numbers of signal and background events and the number of observed candidates are given in Table 1.

For the NN (cut) searches, a total of 134 (95) events are selected in the data, while 128.7 (87.6) events are expected from Standard Model background processes. Figs. 3(a) (NN) and 3(b) (cut) show the distributions of the reconstructed Higgs boson mass for the data and the expected background. Although there is good agreement between the data (dots) and the expected

Table 1
The number of signal and background events expected, and the number of candidate events observed in the year 2000 data. For each channel the systematic error on the background is indicated. The expected background is divided into ZZ (including Ze^+e^- and $Z\nu\bar{\nu}$), WW (including $We\nu$), and $f\bar{f}$ (including $\gamma\gamma \to f\bar{f}$). The expectation for the signal and its significance (Section 3) are computed for a Higgs boson with a mass of 114 GeV/c^2. The numbers from the $H\ell^+\ell^-$ and $\tau^+\tau^-q\bar{q}$ analyses are included in both the NN and cut totals

Analysis	Signal events expected	Background events expected				Events obs.	Expected significance
		ZZ	WW	$f\bar{f}$	Total		(σ)
$Hq\bar{q}$ (NN)	4.5	23.0±1.0	8.6±0.6	15.3±1.7	46.9±2.1	52	1.6
$Hq\bar{q}$ (Cut)	2.9	12.6±0.7	3.2±0.2	7.9±0.7	23.7±1.0	31	1.3
$H\nu\bar{\nu}$ (NN)	1.4	13.5±0.7	22.0±1.1	2.0±0.4	37.5±1.4	38	0.8
$H\nu\bar{\nu}$ (Cut)	1.3	9.9±1.1	8.8±1.7	1.0±0.3	19.7±2.0	20	0.7
$H\ell^+\ell^-$	0.7	26.4±0.3	2.4±0.1	1.8±0.3	30.6±0.4	29	0.8
$\tau^+\tau^-q\bar{q}$	0.4	6.4±0.3	6.2±0.3	1.0±0.3	13.6±0.5	15	0.4
NN total	7.0	69.3±1.3	39.2±1.3	20.1±1.8	128.7±2.6	134	2.1
Cut total	5.3	55.3±1.4	20.6±1.7	11.7±0.9	87.6±2.4	95	1.8

background (histogram) in the total number of events, an excess of data events can be seen in both the NN and cut distributions for large reconstructed Higgs boson masses.

3. Confidence level results

The mass is not the only information which allows Higgs boson production to be distinguished from background. Additional information is taken into account in the likelihood ratio $Q = L_{s+b}/L_b$, where L_b is the likelihood of the background hypothesis, and L_{s+b} is the likelihood when a specific Higgs boson signal is added to the background. The likelihood ratio measures the compatibility of the experiment with a particular signal mass hypothesis:

$$Q = \frac{L_{s+b}}{L_b} = \frac{e^{-(s+b)}}{e^{-b}} \prod_{i=1}^{n_{\text{obs}}} \frac{s f_s(\vec{X}_i) + b f_b(\vec{X}_i)}{b f_b(\vec{X}_i)},$$

where s and b are the total numbers of signal and background events expected. Neglecting the f_s and f_b terms, this is simply the ratio of the Poisson probabilities to observe n_{obs} events for the signal-plus-background and background-only hypotheses. The functions f_s and f_b are the probability densities that a signal or background event will be found in a given final state with the set of values $\vec{X}_i$ which includes the reconstructed mass and possibly a second discriminant.

The four-jet NN analysis uses the neural network output as a second discriminant, while the missing energy NN and lepton pair selections use the sum of the b tagging neural network output values of the hadronic jets as a second discriminant. The four-jet cut, missing energy cut, and tau lepton analyses use only the reconstructed Higgs boson mass as a discriminant.

A small correlation between the neural network output and the reconstructed Higgs boson mass for both the signal and the background distributions was observed in the four-jet NN analysis. The effect of this correlation has been taken into account. No correlation was found between the b tagging distributions and the reconstructed Higgs boson mass in the missing energy NN and lepton pair analyses.

The compatibility of an experiment with a given hypothesis is determined from the expected distribution of the likelihood ratio by calculating the probability of obtaining a likelihood ratio smaller than the one observed. This probability, called the confidence level (CL), depends upon the hypothesized Higgs boson mass for both the signal-plus-background and the

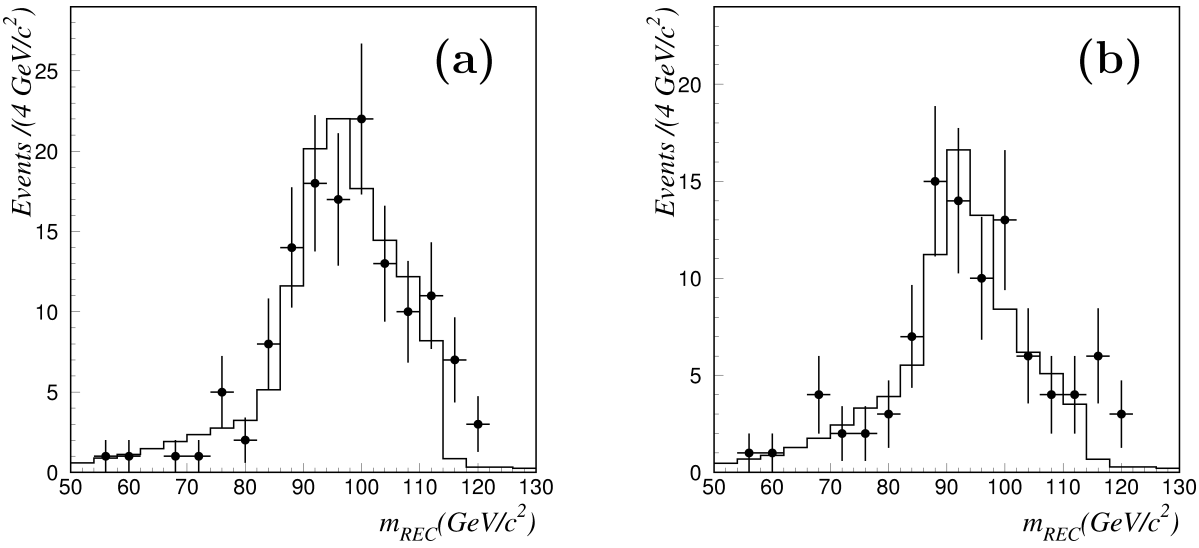

Fig. 3. Distributions of the reconstructed Higgs boson mass for the data collected in 2000 (dots with error bars) and the expected background (histogram) for the (a) NN and (b) cut streams.

background-only hypotheses. If the hypothesis being tested is true, then the distribution of possible confidence levels is equally distributed between 0 and 1, with a median value of 0.5. A signal is expected to produce an excess relative to the expected background, which would appear as a dip in $1 - c_b$, where c_b is the confidence level for the background-only hypothesis.

The $176\,\mathrm{pb}^{-1}$ and $237\,\mathrm{pb}^{-1}$ of data collected in 1998 and 1999 respectively, with centre-of-mass energies ranging from 188.6 GeV to 201.6 GeV, were combined with the data collected in the year 2000 to determine the compatibility of the results with either the background-only or signal-plus-background hypotheses. The observed distribution of $-2\ln Q$ is shown as a function of the hypothesized Higgs boson mass in Figs. 4(a) (NN) and 4(b) (cut). The likelihood ratio is traditionally shown in the form $-2\ln Q$ (the log-likelihood estimator) because of the relationship between the likelihood ratio and chi-squared distributions, and because when the logarithm is taken, individual events contribute as a sum of event weights, $\ln(1 + \frac{sf_s}{bf_b})$, which can be examined individually. The most likely Higgs boson mass corresponds to the minimum, observed near $114\,\mathrm{GeV}/c^2$.

Figs. 5(a) (NN) and 5(b) (cut) show the expected and observed distributions of $1 - c_b$ as a function of the Higgs boson mass. A large deviation from 0.5 can be seen, consistent with an excess over the background hypothesis, which is maximal for a Higgs boson mass of $116\,\mathrm{GeV}/c^2$. The difference between the position of the likelihood ratio and $1 - c_b$ minima is due to the inclusion of the expected signal cross section in the likelihood ratio calculation which, as can be seen in Fig. 2, decreases rapidly with increasing Higgs boson mass. The probability of having such a large excess is 1.5×10^{-3} and 1.1×10^{-3} for the NN and cut streams, respectively. The significance of this excess is 3.0σ and 3.1σ relative to the expected background in the NN and cut streams.[31] The expected significance of the excess for a Higgs boson signal with a mass of $114\,\mathrm{GeV}/c^2$ is shown for each analysis in Table 1.

The Signal Estimator method [10] is used to derive a 95% CL lower limit on the Standard Model Higgs boson mass of $111.1\,\mathrm{GeV}/c^2$ ($110.6\,\mathrm{GeV}/c^2$) with an expected limit of $114.2\,\mathrm{GeV}/c^2$ ($113.8\,\mathrm{GeV}/c^2$) for the NN (cut) stream.

[31] The LEP Higgs Working Group has adopted a different convention, using a double-sided Gaussian distribution, which gives a significance of 3.2σ instead of 3.0σ for the NN analysis and 3.3σ instead of 3.1σ for the cut analysis [9].

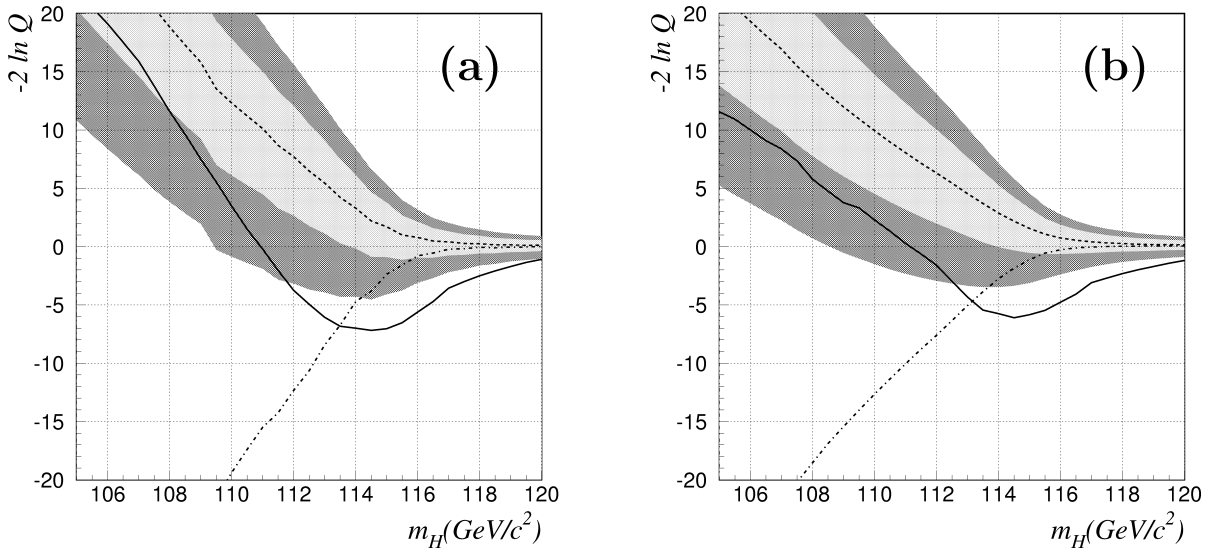

Fig. 4. The log-likelihood estimator $-2\ln Q$ for the (a) NN and (b) cut streams as a function of the mass of the Higgs boson for the observation (solid) and background-only expectation (dashed). The light and dark grey regions around the background expectation represent the one and two sigma bands, respectively. The dash-dotted curves show the medians of the log-likelihood estimator as a function of the Higgs boson mass for the signal hypothesis.

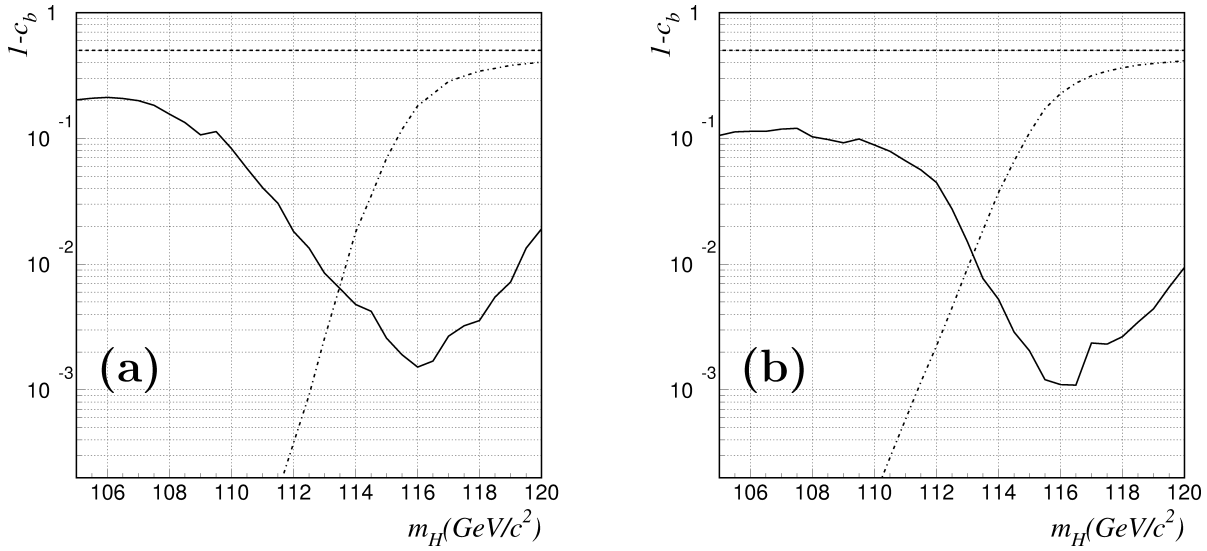

Fig. 5. Observed (solid) and expected (dashed) CL curves for the background hypothesis as a function of the hypothesized Higgs boson mass for the (a) NN and (b) cut streams. The dash-dotted curves indicate the location of the median CL for a Higgs boson signal as a function of the Higgs boson mass.

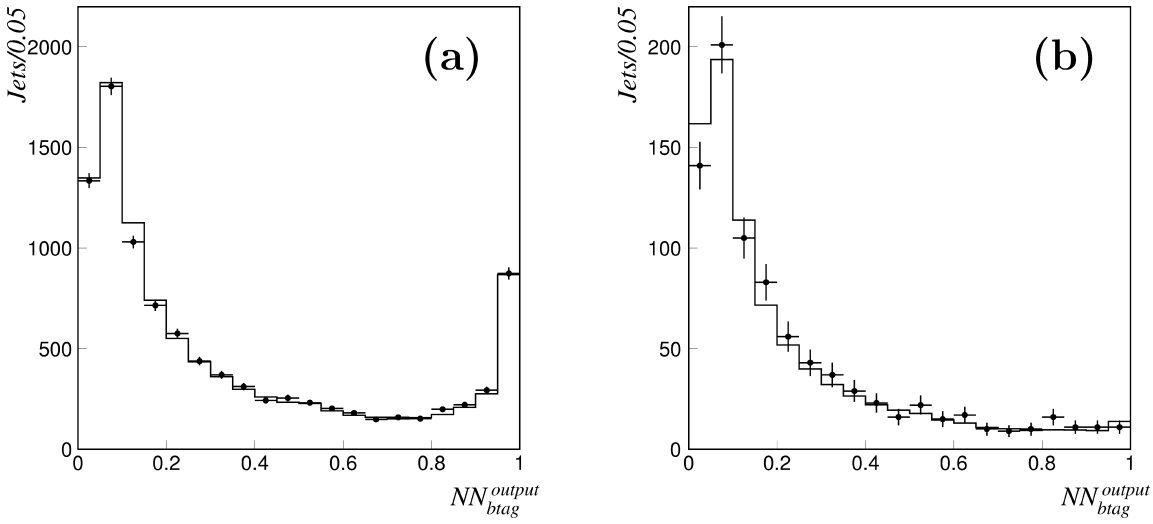

Fig. 6. Distribution of the b tagging neural network output for jets from (a) radiative Z return events and (b) semileptonic W^+W^- events, in the data (dots with error bars) and the simulation (histogram).

4. Systematic uncertainties

Systematic uncertainties in the simulation were evaluated in a similar manner to Ref. [8] and are summarized for the expected backgrounds in Table 1. The systematic uncertainty in the expected number of signal events is typically less than 5%.

Whenever possible, the systematic uncertainties were extracted from $3.2\,\mathrm{pb}^{-1}$ of data taken at the Z peak during the same year. As in previous years, a slight discrepancy between data and simulation was observed in the impact-parameter-based b tagging quantities. To correct for this effect, a smearing of the track parameters was performed on the simulated events to bring them into better agreement with the data. Half of the correction was taken as a systematic uncertainty. Fig. 6 shows good agreement between the high energy data and the simulation for both (a) the radiative Z return events, which in 22% of the cases contain b quark jets, and (b) the semileptonic W^+W^- events containing essentially udsc quarks.

The reconstruction of the jet energies and angles has also been studied with the Z peak data, using the method described in Ref. [8]. The small differences between data and simulation are taken into account by smearing the jets in the simulated events; half of this correction is taken as a systematic uncertainty.

Uncertainties in the distributions of the discriminants used in the likelihood ratio are dominated in most analyses by the statistical uncertainties of the simulated samples.

The high mass excess could indicate a possible bias in the mass reconstruction, not reproduced in the simulation, which would preferentially select events near the kinematic limit $m_{\mathrm{H}} \approx \sqrt{s} - m_{\mathrm{Z}}$. The excess is mainly in the $131\,\mathrm{pb}^{-1}$ of data with centre-of-mass energies greater than 206 GeV. To investigate the possibility a bias, the number of selected events with reconstructed masses within $5\,\mathrm{GeV}/c^2$ of the kinematic limit were determined for the four-jet analyses in the 1999 and 2000 data. For $322\,\mathrm{pb}^{-1}$ of data with centre-of-mass energies below 206 GeV, 11 (4) events were selected with 8.9 (4.6) background events expected from the NN (cut) analyses. While for the $131\,\mathrm{pb}^{-1}$ of data with $\sqrt{s} > 206\,\mathrm{GeV}$, 7 (6) events are selected with 3.5 (1.8) background events expected. As the four-jet analyses and the event simulations are unchanged since 1999, there is no evidence of a bias towards the kinematic limit.

To illustrate the reliability of the mass reconstruction, Fig. 7 shows the reconstructed Higgs boson mass distribution from the four-jet cut analysis after all kinematic cuts are applied and also requiring that no jet has a b tagging neural network output value greater than

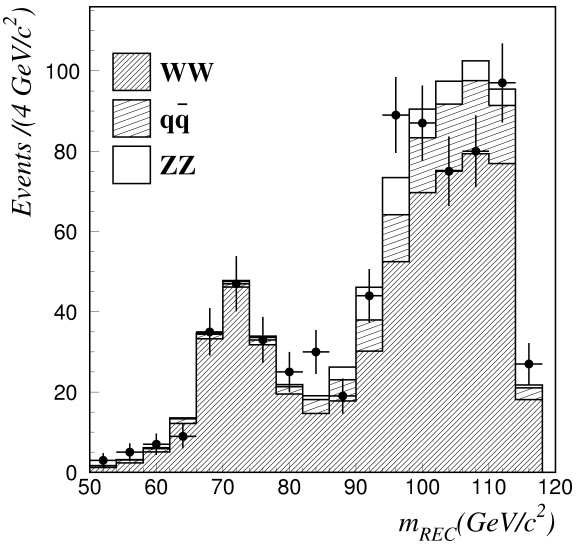

Fig. 7. Reconstructed Higgs boson mass distribution of the four-jet cut analysis with all kinematic cuts applied and requiring that no jet has a b tagging neural network output value greater than 0.9. The data are shown as the dots with error bars and the simulation, dominated by W^+W^- events, is the histogram.

0.9. No indication of a non-simulated bias is seen in the reconstructed mass distribution. The background is dominated by W^+W^- events; the lower mass peak corresponds to $2m_W - m_Z$, while the broad contribution at high masses is mostly due to W^+W^- events with a wrong pairing assignment.

As the systematic effects are still under investigation, the confidence level calculations reported in this letter do not include the systematic uncertainties. An estimate of the impact of these uncertainties has been made by simultaneously increasing the numbers of expected background events by their errors (Table 1). The significance of the excess is then reduced by 0.2σ. The uncertainty on the distribution of the discriminants is estimated to have an even smaller effect.

5. Impact of individual events

In order to determine the impact of any given candidate event on the excess, its "weight", i.e., its contribution to the logarithm of the likelihood ratio, is calculated as a function of the Higgs boson mass. In Fig. 8, the event weights are displayed as a function of the assumed Higgs boson mass for those events with weights larger than 0.4 at a mass of $114\,\mathrm{GeV}/c^2$.

Details of the five four-jet events with weights larger than 0.4 in either the NN or cut analysis are given in Table 2. All of these events were selected with a centre-of-mass energy greater than 206 GeV. Events *a*, *b*, *c*, and *d* are retained in both the NN and cut analyses, while event *e* has a weight larger than 0.4 only in the cut analysis. The largest contribution to the excess in the NN stream (Fig. 8(a)) comes from three four-jet events (*a*, *b*, and *c*) which have neural network output values larger than 0.99. The four-jet cut analysis uses only the reconstructed Higgs boson mass as discriminant, which causes the three $114\,\mathrm{GeV}/c^2$ events (*c*, *d*, and *e*) to receive the same weights. The events with lower reconstructed Higgs boson masses (*a* and *b*) have larger weights because they are selected in the higher purity 4b final state.

The set of events with weights larger than 0.4 at $114\,\mathrm{GeV}/c^2$ contains two more events, one in the lepton pair final state and one in the tau pair final state, which belong to both analysis streams. No such high weight events are selected by the missing energy analyses.

The lepton pair final state candidate, recorded at $\sqrt{s} = 205\,\mathrm{GeV}$, is shown as the dashed curve in Figs. 8(a) and 8(b). It is reconstructed with a Higgs boson mass of $118\,\mathrm{GeV}/c^2$ and a b tagging neural network sum of 1.4 for the two Higgs boson jets. The invariant mass of the e^+e^- pair is $78.8\,\mathrm{GeV}/c^2$. The electron in the event is 6° away from one of the hadronic jets. Because the analysis does not correct for bremsstrahlung photons for electrons within 10° of any jet, 18 GeV of neutral electromagnetic energy within 2° of the electron is not considered as bremsstrahlung energy. If this energy were added to the leptonic system, its mass would increase to $93.3\,\mathrm{GeV}/c^2$ and the reconstructed Higgs boson mass would decrease to $99.5\,\mathrm{GeV}/c^2$.

The $H\tau^+\tau^-$ candidate, recorded at $\sqrt{s} = 208$ GeV, is shown as the dotted curve in Figs. 8(a) and 8(b). It has a reconstructed Higgs boson mass of $115\,\mathrm{GeV}/c^2$. The tau leptons are well isolated and the Higgs boson jets are well b tagged. The quality of the kinematic fit is however poor, which is not reflected in the event weight since only the reconstructed mass is used as discriminant.

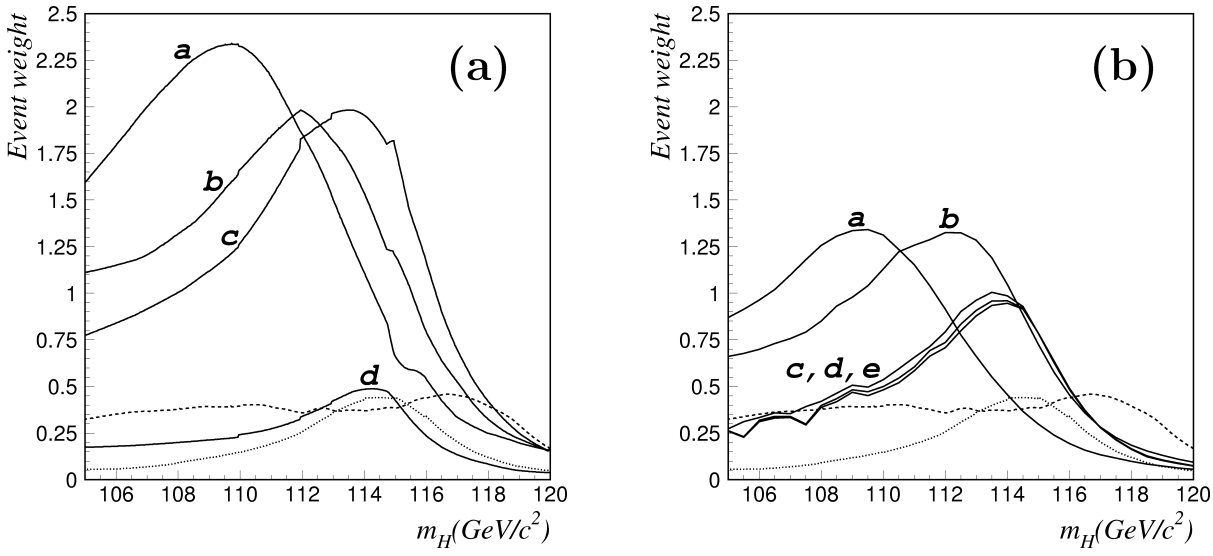

Fig. 8. Event weight of each candidate as a function of the Higgs boson mass for the four-jet (solid), lepton pair (dashed) and tau pair (dotted) final state candidates with a weight larger than 0.4 at a mass of $114\,\mathrm{GeV}/c^2$ in the (a) NN and (b) cut streams.

Table 2
Details of the five four-jet candidates selected with an event weight greater than 0.4 at a Higgs boson mass of $114\,\mathrm{GeV}/c^2$ in either the NN or cut streams. The Higgs boson mass is calculated as $m_{12} + m_{34} - 91.2\,\mathrm{GeV}/c^2$, where jets 3 and 4 are the Higgs boson jets

Candidate	Higgs mass	m_{12}	m_{34}	B tagging				4-Jet
(run/event)	(GeV/c^2)	(GeV/c^2)	(GeV/c^2)	Jet 1	Jet 2	Jet 3	Jet 4	NN
a (56698/7455)	110.0	96.3	104.9	0.999	0.836	0.999	0.214	0.999
b (56065/3253)	112.9	94.9	109.2	0.994	0.776	0.993	0.999	0.997
c (54698/4881)	114.3	101.3	104.2	0.136	0.012	0.999	0.999	0.996
d (56366/0955)	114.5	78.8	126.9	0.238	0.052	0.998	0.948	0.935
e (55982/6125)	114.6	79.7	126.1	0.088	0.293	0.895	0.998	0.820

6. High purity candidates

The stability of the excess can be investigated by increasing the purity of the event selections. The selection criteria of all analyses are tightened to give a signal ($m_H = 114\,\mathrm{GeV}/c^2$) to background ratio ($s/b$) of 1.5 for events with a reconstructed Higgs boson mass greater than $109\,\mathrm{GeV}/c^2$. Figs. 9(a) and 9(b) show the high purity distributions of the reconstructed Higgs boson mass for the NN and cut streams, respectively. To obtain a high purity selection in the four-jet NN analysis, the cut on the neural network output is tightened. The purity of the four-jet cut selection is increased by tightening cuts on the b tagging and the fitted Z boson mass, m_{12}. In the high mass region above $109\,\mathrm{GeV}/c^2$, both the NN and cut streams select the same events, namely the three four-jet candidates a, b, and c. Two of the $114\,\mathrm{GeV}/c^2$ candidates (d and e) significantly affecting the excess in the cut stream are removed by the tighter cut on m_{12}. In this high mass region, 0.9 (0.6) background events are expected, equally composed of $\mathrm{q\bar{q}}$ and ZZ events,

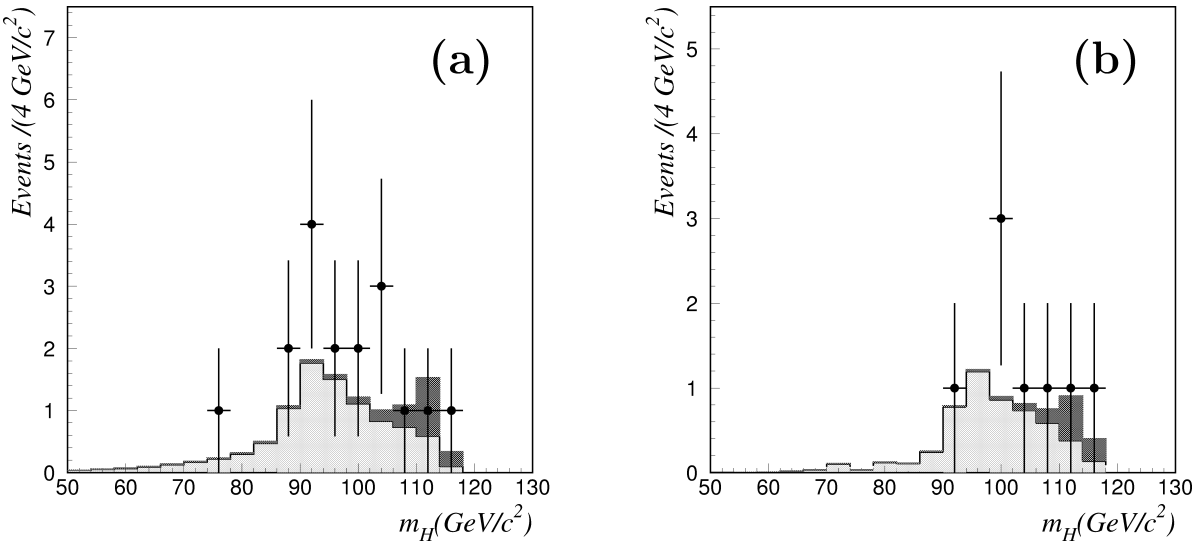

Fig. 9. High purity ($s/b = 1.5$) reconstructed Higgs boson mass distributions for the (a) NN and (b) cut selections for the data (dots with error bars), the expected background (light histogram), and the expected signal with a Higgs boson mass of 114 GeV/c^2 (dark histogram).

while 1.3 (0.9) signal events ($m_H = 114\,\mathrm{GeV}/c^2$) are expected for the NN (cut) stream, all in the four-jet topology.

The three high purity four-jet candidates were reprocessed with the event reconstruction program taking into account all of the final detector calibrations and alignments. The changes in the reconstructed Higgs boson masses and neural network values for all three candidates are insignificant.

Candidate a

The first high purity candidate (*a* shown in Fig. 10), at a centre-of-mass energy of 206.6 GeV, is reconstructed with a Higgs boson mass of 110.0 GeV/c^2. Three of the four jets are well b tagged and the event is selected as a 4b event [8] with the sum of the four b tagging neural network output values equal to 3.05. The lowest b tagged jet with a value of 0.214 is selected as one of the Higgs boson jets. The probability for any jet in a 4b event to have such a low b tagging value is 19%.

As the event is identified as a 4b event, any of the six possible pairing combinations can be considered in its interpretation. The pairing most compatible with the ZZ hypothesis, using a fit including the Z boson width and mass resolutions, gives large fitted Z boson masses of 98.9 GeV/c^2 and 101.6 GeV/c^2.

Candidate b

The second high purity candidate (*b*), shown in Fig. 11, has a reconstructed Higgs boson mass of 112.9 GeV/c^2. All four of the jets in the event are well b tagged with a b tagging neural network sum of 3.76. The measured visible energy in this event is 252 GeV, which is much larger than that allowed by the energy resolution of about 10 GeV for an event with a centre-of-mass energy of 206.7 GeV. A 22 GeV electromagnetic shower is detected in the small angle calorimeter (SICAL) in the plane of the accelerator. As there is too much reconstructed energy and the momentum imbalance is in the opposite direction to the 22 GeV energy deposit, this shower is most likely a beam-related particle, unrelated to the rest of the event. Although the overlapping of such beam-related background is not frequent, the 22 GeV of energy is consistent with the observation in events triggered at random beam crossings, as can be seen in Fig. 12.

If this low-angle energy deposit is removed from the event, the reconstructed Higgs boson mass increases from 112.9 GeV/c^2 to 114.5 GeV/c^2. The neural net-

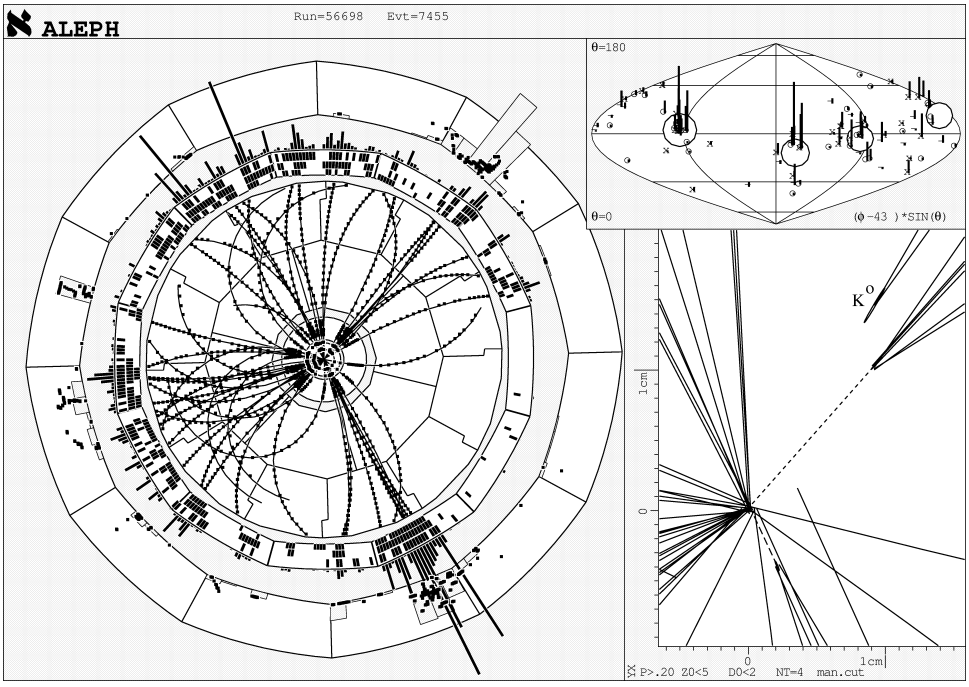

Fig. 10. Four-jet Higgs boson candidate (a) with a reconstructed Higgs boson mass of 110.0 GeV/c^2. Three of the four jets are well b tagged. The event is shown in the view transverse to the beam direction, the θ-ϕ sinθ view, and in a closeup of the charged particles in the vertex region.

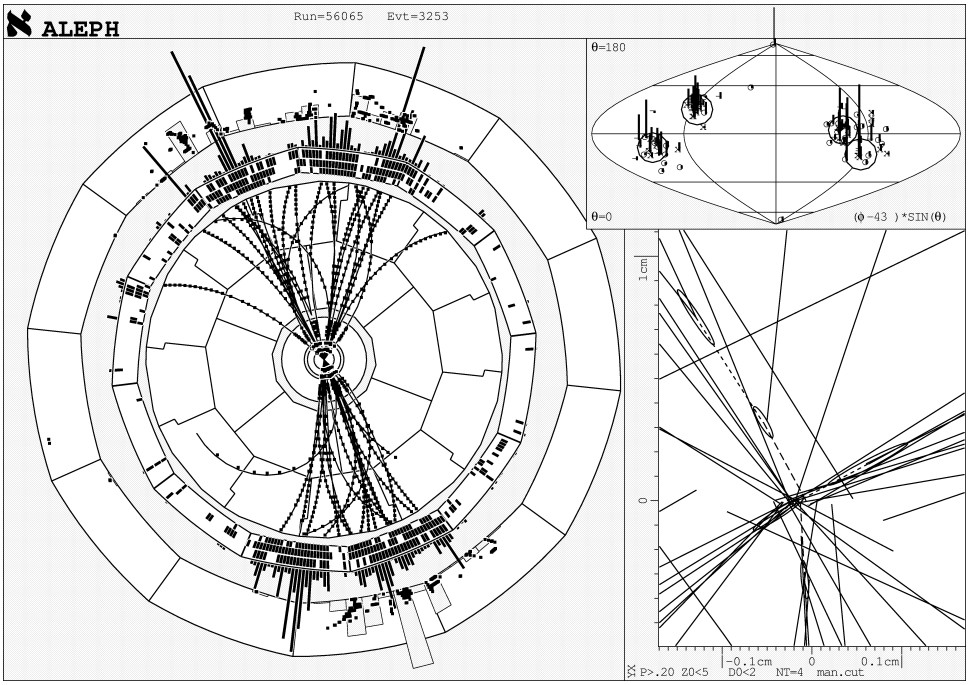

Fig. 11. Four-jet Higgs boson candidate (b) with a reconstructed Higgs boson mass of 112.9 GeV/c^2. All four jets are well b tagged.

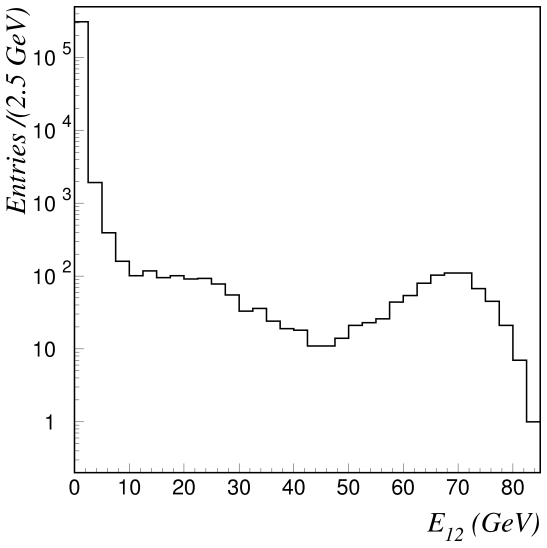

Fig. 12. Energy distribution of the most energetic electromagnetic particle within 12° of the beam in events triggered at random beam crossings.

work output for this event is stable and changes from 0.997 to 0.998. Because the reconstructed Higgs boson mass shifts closer to the excess, the significance of the excess would increase by $0.2\,\sigma$ for both the NN and cut streams.

Even if the 22 GeV particle is removed from the event, there is still an energy excess of 23.3 GeV indicating a mismeasurement of jet energy. Such a mismeasurement is often due to fake neutral hadrons, i.e., hadronic showers which should have been assigned to a charged particle. This causes double counting in the computation of the energy of the jet. Indeed the detailed inspection of one of the jets shows that a 13 GeV neutral hadron is likely to have been misidentified. If this object is removed from the jet and the Higgs boson mass recomputed, excluding at the same time the low angle (SICAL) object, a value of $114.2\,\mathrm{GeV}/c^2$ is obtained. The very small variation in the reconstructed Higgs boson mass occurs because the fitted masses depend more strongly on the measured jet directions than on the jet energies.

As for the first high purity 4b candidate (a), the best background explanation for this event is the ZZ hypothesis with a different jet pairing. The Z boson masses from a fit for the most probable ZZ pairing choice are $94.0\,\mathrm{GeV}/c^2$ and $97.3\,\mathrm{GeV}/c^2$.

Candidate c

The third high purity four-jet candidate (c), at a centre-of-mass energy of $206.7\,\mathrm{GeV}/c^2$, has a reconstructed Higgs boson mass of $114.3\,\mathrm{GeV}/c^2$. Both of the Higgs boson jets are very well b tagged with well measured displaced vertices and b tagging neural net values of 0.999. The $13.8\,\mathrm{GeV}/c$ of missing momentum in the event points to the middle of the Higgs boson jet containing an identified muon coming from the secondary vertex, as shown in Fig. 13. This is a strong indication that, except for the unmeasured neutrino from the semileptonic b quark decay, the rest of the event is well measured. This is also supported by the fact that the measured invariant mass of the two non b tagged jets is $92.1\,\mathrm{GeV}/c^2$, consistent with a Z boson. The measured invariant mass of the b tagged jets and the missing momentum is $114.4\,\mathrm{GeV}/c^2$, which renders unlikely the ZZ hypothesis.

Due to the low value of the smallest angle between the four jets (37°), the most likely background explanation for this event is the $b\bar{b}gg$ hypothesis. The minimum jet-jet angle for the $b\bar{b}gg$ background peaks at low values with 42% of the events having angles less than 37°, while 11% of the signal events have such a low angle. The two measured jet energies of the non-b jets, 43.5 GeV and 49.0 GeV, are typical, however, for the decay of a Z boson produced nearly at rest.

7. Conclusions

The data collected with the ALEPH detector at centre-of-mass energies up to 209 GeV have been analysed to search for the Standard Model Higgs boson. The search was performed using both a neural-network-based stream and a cut-based stream. Both analysis streams show a $3\,\sigma$ excess beyond the background expectation, which is largely due to candidate events selected in the four-jet analyses at centre-of-mass energies greater than 206 GeV. The observation is consistent with the production of a Higgs boson with a mass near $114\,\mathrm{GeV}/c^2$. Reprocessing the most significant candidates using the final calibration and varying the background expectation by the systematic uncertainties has shown that these results are stable.

Results from the four LEP experiments on the search for the Standard Model Higgs boson were

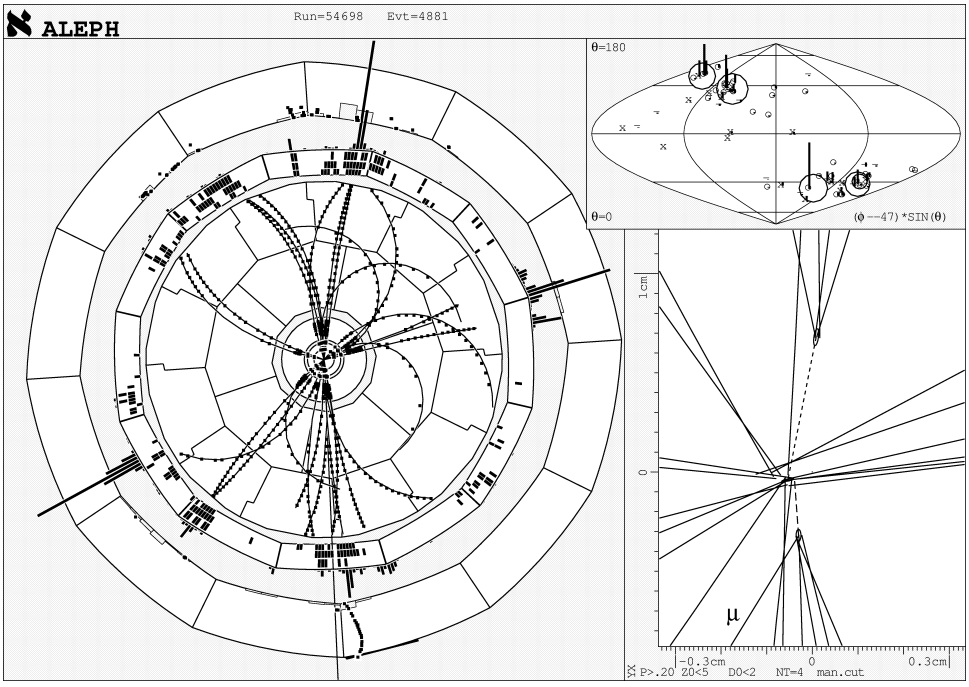

Fig. 13. Four-jet Higgs boson candidate (c) with a reconstructed Higgs boson mass of $114.3\,\mathrm{GeV}/c^2$. The two Higgs boson jets are well b tagged.

shown at the LEPC meeting on November 3, 2000 [11]. More data, or results from other experiments, will be needed to determine whether the observations reported in this Letter are the result of a statistical fluctuation or the first sign of direct production of the Higgs boson.

Acknowledgements

We congratulate our colleagues from the accelerator divisions for the very successful running of LEP at high energies. Without the extraordinary achievement of operating LEP at energies much above the design value, these observations would not have been possible. We are indebted to the engineers and technicians in all our institutions for their contribution to the excellent performance of ALEPH. Those of us from non-member countries thank CERN for its hospitality.

References

[1] P.W. Higgs, Phys. Lett. 12 (1964) 132;
P.W. Higgs, Phys. Rev. Lett. 13 (1964) 508;
P.W. Higgs, Phys. Rev. 145 (1966) 1156;
F. Englert, R. Brout, Phys. Rev. Lett. 13 (1964) 321;
G.S. Guralnik, C.R. Hagen, T.W.B. Kibble, Phys. Rev. Lett. 13 (1964) 585;
T.W.B. Kibble, Phys. Rev. 155 (1967) 1554.

[2] ALEPH Collaboration, Searches for neutral Higgs bosons in e^+e^- collisions at centre-of-mass energies from 192 to 202 GeV, CERN-EP/2000-131, 2000, submitted to Phys. Lett. B.

[3] ALEPH Collaboration, ALEPH: A detector for electron–positron annihilations at LEP, Nucl. Instrum. Methods A 294 (1990) 121;
ALEPH Collaboration, Performance of the ALEPH detector at LEP, Nucl. Instrum. Methods A 360 (1995) 481;
D. Creanza et al., The new ALEPH vertex detector, Nucl. Instrum. Methods A 409 (1998) 157.

[4] J. Ellis, M.K. Gaillard, D.V. Nanopoulos, A phenomenological profile of the Higgs boson, Nucl. Phys. B 106 (1976) 292;
B.L. Ioffe, V.A. Khoze, What can be expected from experiments on colliding e^+e^- beams with energy approximately

equal to 100 GeV, LENINGRAD-76-274 (1976), Sov. J. Part. Nucl. 9 (1978) 50;
B.W. Lee, C. Quigg, H.B. Thacker, Weak interactions at very high energies: the role of he Higgs boson mass, Phys. Rev. D 16 (1977) 1519;
J.D. Bjorken, Weak interaction theory and neutral currents, in: M.C. Zipf (Ed.), Proc. of the 1976 SLAC Summer Inst. on Particle Physics, SLAC report 198, 1977, p. 1;
F.A. Berends, R. Kleiss, Initial state radiation at LEP energies and corrections to Higgs boson production, Nucl. Phys. B 260 (1985) 32.

[5] W. Kilian, M. Kramer, P.M. Zerwas, Higgsstrahlung and WW fusion in e^+e^- collisions, Phys. Lett. B 373 (1996) 135;
W. Kilian, M. Kramer, P.M. Zerwas, Higgsstrahlung and vector boson fusion in e^+e^- collisions, hep-ph/9605437, 1996.

[6] ALEPH Collaboration, Search for the neutral Higgs bosons of the MSSM in e^+e^- collisions at $\sqrt{s}$ from 130 to 172 GeV, Phys. Lett. B 412 (1997) 173.

[7] S. Catani et al., New clustering algorithm for multi-jet cross-sections in e^+e^- annihilation, Phys. Lett. B 269 (1991) 179;
N. Brown, J. Stirling, Finding jets and summing soft gluons: A new algorithm, Z. Phys. C 53 (1992) 629.

[8] ALEPH Collaboration, Search for the neutral Higgs bosons of the Standard Model and the MSSM in e^+e^- collisions at $\sqrt{s} = 189$ GeV, CERN-EP/2000-019, 2000, to be published in Eur. Phys. J. C.

[9] D.E. Groom et al., Review of particle physics, Eur. Phys. J. C 15 (2000) 1.

[10] S. Jin, P. McNamara, The signal estimator limit setting method, physics/9812030, to be published in Nucl. Instrum. Methods A.

[11] P. Igo-Kemenes, Status of the Higgs boson searches, November 3, 2000, LEPC presentation, http://lephiggs.web.cern.ch/LEPHIGGS/talks/index.html.